Iraqi Journal of Physics, 2015 *Vol.13, No.26, PP. 112-120*

Nuclear structure study of some tin isotopes using the self-consistent mean field method

Ali A. Alzubadi, Mohammed F. Majid

Physics Department, College of Science, University of Baghdad, Baghdad, Iraq.

E-mail: alwassity@ymail.com

Abstract

Hartree-Fock calculations for even-even Tin isotopes using Skyrme density dependent effective nucleon-nucleon interaction are discussed systematically. Skyrme interaction and the general formula for the mean energy of a spherical nucleus are described. The charge and matter densities with their corresponding rms radii and the nuclear skin for Sn isotopes are studied and compared with the experimental data. The potential energy curves obtained with inclusion of the pairing force between the like nucleons in Hartree-Fock-Bogoliubov approach are also discussed.

Key words

Mean field, Skyrme-Hartree-Fock, Hartree-Fock-Bogoliubov, Pairing force.

Article info.

Received: Oct. 2014
Accepted: Nov. 2014
Published: Apr. 2015

دراسة التركيب النووي لبَعْض نظائر القصدير بِطريقَة معدل المجال المولد ذاتيا

علي عبد اللطيف الزبيدي، محمد فالح ماجد

قسم الفيزياء، كلية العلوم، جامعة بغداد، بغداد، العراق.

الخلاصة

نوقشت حسابات هارتري-فوك لنظائر القصدير الزوجية-زوجية بالأستعانة بتفاعل سكيرم المعتمد على الكثافة بين كل نيوكلونين، ثم تم وصف تفاعل سكيرم والصيغة العامة لمعدل الطاقة للنوى الكروية. وكذلك درست الكثافة النووية وكثافة الشحنة وجذر معدل مربع نصف القطر والغلاف النووي مقارنة بنتائج القيم العملية. اضافة الى ذلك تمت مناقشة منحنيات الطاقة الكامنة بأستخدام تفاعل الازدواج بين النيوكلونات المتشابهة في حسابات هارتري-فوك-بوكليوبوف.

Introduction

Microscopic theories using the mean field (MF) approximation have been gaining, year after year, a high level of reliability for the description of static and dynamic properties of atomic nuclei. Reasonable theoretical predictions can now be expected to explain the properties of nuclei not only in their ground states but also in extreme conditions of spin or isospin far away from the normal stability of the nuclear matter [1].

The MF methods are very successful in describing and predicting properties of nuclei across the chart of the nuclides. This is especially true for heavy nuclei, where the bulk properties of nuclear mater dominate over the surface effects. However, when details of nuclear structure are considered, a correct description of the nuclear surface is essential. Moreover, the surface region may give us invaluable information on the nature and strength of nuclear effective interaction in channels that are inaccessible by considering infinity systems (i.e., nuclear matter) [2].

Static properties essentially involve ground states of nuclei (binding energies,

radii, separation energies of one or two nucleons, shell effects…) and are well described within Hartree-Fock (HF) or Hartree-Fock-Bogoliubov (HFB) approaches including pairing correlations. Dynamic properties more generally affect the excited states (single or collective excitations, giant resonances, fission…) for which it is necessary to go beyond the MF approximation in order to obtain a correct description of experimental data. These methods, such as the random phase approximation [1] or the generator coordinate method; perform a particular mixing of configurations. And to be consistent they are all based on a set of wavefunctions issued from a MF calculation and in this way they can be generated as successive approximations of the general Time-Dependent HF formalism [1].

Microscopic MF theories are based on the fundamental assumption that neutrons and protons inside the nucleus are moving independently from each other under the influence of a potential averaging their interactions. This approximation finds a steady experimental verification for instance in the shell model framework and the occurrence of magic numbers. A simple calculation [3] enables to justify this approximation when evaluating the mean free path (defining as the least distance between two collisions of a nucleon inside the nucleus) which turns out to be several times larger than the size of the nucleus. The explanation of this result is that the Pauli principle limits strongly the possible final states in case of nucleon-nucleon (NN) collisions in the nucleus [4]. As a matter of fact a nucleon does not see the other ones but only feels the average potential which retains it inside the nucleus. Beside the shell model, a MF theory enables to derive the nuclear MF microscopically.

The determination of the nuclear skin thickness usually involves the precise measurement of the root mean square (rms) radii of both charge and mass distributions. Calculations of nuclear charge and matter radii of nuclei are usually made in the framework of MF approaches, namely, the HF method or the HFB method including pairing correlations. We will use different Skyrme parameterizations, which can give an appropriate description of bulk properties of even-even nuclei.

Theoretical consideration

The self-consistent deformed HF calculations with density-dependent Skyrme interactions [5] and pairing correlations are discussed as follows. In its original form, Skyrme interaction can be written as a potential,

$$V = \sum_{i<j} v_{ij} + \sum_{i<j<k} v_{ijk}, \qquad (1)$$

with a two-body part v_{ij} and three-body part v_{ijk}. To simplify calculations, Skyrme used a short range expansion for the two-body interaction. The matrix elements in momentum space are [6],

$$\left\langle \vec{k} \left| v_{12} \right| \vec{k}' \right\rangle = t_o\left(1+x_o P_\sigma\right)+\frac{1}{2}t_1\left(k^2+k'^2\right) + t_2\vec{k}\cdot\vec{k}'+iw_o\left(\vec{\sigma}_1+\vec{\sigma}_2\right)\cdot\vec{k}\times\vec{k}', \qquad (2)$$

The terms t_0, t_1, t_2, x_0 and w_0 are the free parameters describing the strengths of the different interaction terms which are fitted to the nuclear structure data, and the operators $\vec{k}$ and $\vec{k}'$ are relative wave vectors of two nucleons, $\vec{k}$ denotes the operator $(\vec{\nabla}_1 - \vec{\nabla}_2)/2i$ acting on the right; whereas, $\vec{k}'$ is the operator $-(\vec{\nabla}_1 - \vec{\nabla}_2)/2i$ acting on the left. P_σ is a spin exchange operator and the $\vec{\sigma}$is Pauli spin matrix. To see how one deals with such an interaction in practical calculation it is convenient to write it in configuration space.

The Skyrme interaction can be expressed as:

$$
\begin{aligned}
v_{12} &= t_o\left(1+x_o\hat{p}_\sigma\right)\delta\left(r_1-r_2\right)\\
&+\frac{t_1}{2}\left(1+x_1\hat{p}_\sigma\right)\left(\hat{k}'^2\delta\left(r_1-r_2\right)+\delta\left(r_1-r_2\right)\hat{k}^2\right)\\
&+t_2\left(1+x_2\hat{p}_\sigma\right)\hat{k}'.\delta\left(r_1-r_2\right)\hat{k}\\
&+\frac{t_3}{6}\left(1+x_3\hat{p}_\sigma\right)\rho^\alpha\left(R\right)\delta\left(r_1-r_2\right)\\
&+iw_o\hat{k}'\left(\hat{\sigma}_1+\hat{\sigma}_2\right)\times\hat{k}\,\delta\left(r_1-r_2\right). \qquad (3)
\end{aligned}
$$

By considering the matrix elements of above expression in a state of relative motion $\Psi(\vec{r}) = R(r)Y_{lm}(\Omega)$, one can see that the matrix element of the first two terms (which are corresponding to S-wave interaction) are proportional to $|\Psi(0)|^2$ and $\Psi(0)\nabla^2\Psi(0)$, respectively, and the matrix elements of the last two teams (which are corresponding to P-wave interactions) are proportional to $|\vec{\nabla}\Psi(0)|^2$ [6]. For the Skyrme interaction there exists a very simple way of deriving the HF method, the ground state wavefunction of the nucleus is approximated by a Slater determinant (SD) built on single-particle wavefunctions within the independent particle picture [7]:

$$\Psi_{HF}\left(r_1,\ldots,r_A\right)=\frac{1}{\sqrt{A!}}Det\left\{\phi_{\alpha1}\left(r_1\right).\phi_{\alpha2}\left(r_2\right).\ldots.\phi_{\alpha A}\left(r_A\right)\right\}. \qquad (4)$$

where $\phi_{\alpha i}$ represent the single particle wave function, the number of single particle states is given by the total number of particles in the nucleus, A, where they will be characterized according to their quantum numbers. The expectation value of the HF Hamiltonian or total energy of the system is given by [5]:

$$\left\langle\phi\middle|\hat{H}\middle|\phi\right\rangle=\sum_{i=1}^{A}\left\langle i\middle|\hat{t}\middle|i\right\rangle+\frac{1}{2!}\sum_{ij}^{A}\left\langle ij\middle|\bar{v}_{12}\middle|ij\right\rangle, \qquad (5)$$

The first term represents the kinetic and the second term represents the potential energy, where $\bar{v}_{12}$ indicates the necessity to account for the anti-symmetric nature of the NN interaction, where:

$$\bar{v}_{12}=v_{12}-v_{21}\,. \qquad (6)$$

The use of exchange operators for the position, spin, and isospin accounts for the antisymmetrisation, allowing the use of v_{12} rather than $\bar{v}_{12}$ as [8]:

$$
\begin{aligned}
\hat{P}_M\,\Psi\left(r_1,r_2\right)&=\Psi\left(r_2,r_1\right),\\
\hat{P}_\sigma&=\frac{1}{2}\left(1+\hat{\sigma}_1.\hat{\sigma}_2\right), \qquad (7)\\
\hat{P}_q&=\frac{1}{2}\left(1+\hat{q}_1.\hat{q}_2\right),
\end{aligned}
$$

where $\hat{P}_M$, is the Majorana exchange operator, $\hat{P}_\sigma$ and $\hat{P}_q$ are the position, spin-exchange and isospin operators respectively. The full expectation value of the Hamiltonian is therefore re-written as [6]:

$$
\begin{aligned}
\left\langle\Psi\middle|\hat{H}\middle|\Psi\right\rangle&=\sum_{i=1}^{A}\int d\vec{r}_1\phi_i^*\left(r_1\right)\left(\frac{\hbar^2}{2m}\nabla_i^2\right)\phi_i\left(r_1\right)\\
&+\frac{1}{2}\sum_{ij\sigma_1\sigma_2q_1q_2}\iint d^3r_1\,d^3r\,\phi_i^*\left(r_1,\sigma_1,q_1\right)\phi_j^*\left(r_2,\sigma_2,q_2\right)\\
&v\left(r_1,r_2\right)\left(1-\hat{P}_M\hat{P}_\sigma\hat{P}_q\right)\phi_i\left(r_2,\sigma_2,q_2\right)\phi_j\left(r_2,\sigma_2,q_2\right). \qquad (8)
\end{aligned}
$$

For the Skyrme interaction the energy density $H(\vec{r})$ is an algebraic function of the nucleon densities $\rho_n(\rho_p)$, the kinetic energy $\tau_n(\tau_p)$, and spin densities $\vec{J}_n(\vec{J}_p)$. These quantities depending on the single-particle states ϕ_α defining in the SD wave function.

$$
\begin{aligned}
\rho_q\left(\vec{r}\right)&=\sum_{i\sigma}\left|\phi_i\left(\vec{r},\sigma,q\right)\right|^2,\\
\tau_q\left(\vec{r}\right)&=\sum_{i\sigma}\left|\vec{\nabla}\phi_i\left(\vec{r},\sigma,q\right)\right|^2, \qquad (9)\\
\vec{J}_q\left(\vec{r}\right)&=\left(-i\right)\sum_{i\sigma\sigma'}\phi_i^*\left(\vec{r},\sigma,q\right)\left[\vec{\nabla}\phi_i\left(\vec{r},\sigma',q\right)\times\left\langle\sigma\middle|\vec{\sigma}\middle|\sigma'\right\rangle\right],
\end{aligned}
$$

the sums in the above equations are taken over all occupied single-particle states. The expression for $H(\vec{r})$ was derived. Assuming that the subspace of occupied single-particle states is invariant under time reversal (which implies an even-even nucleus) one gets the following result:

$$H(\vec{r})=\frac{\hbar^2}{2m}\tau(\vec{r})+\frac{1}{2}t_o\left[\left(1+\frac{1}{2}x_o\right)\rho^2-\left(x_o+\frac{1}{2}\right)\left(\rho_n^2+\rho_p^2\right)\right]$$
$$+\frac{1}{4}(t_1+t_2)\rho\tau+\frac{1}{8}(t_2-t_1)\left(\rho_n\tau_n+\rho_p\tau_p\right)+\frac{1}{16}(t_2-3t_1)\rho\nabla^2\rho$$
$$+\frac{1}{32}(t_2+3t_1)\left(\rho_n\nabla^2\rho_n+\rho_p\nabla^2\rho_p\right)+\frac{1}{16}(t_1-t_2)\left(\vec{J}_n^2+\vec{J}_p^2\right)$$
$$+\frac{1}{4}t_3\rho_n\rho_p\rho+H_C(\vec{r})-\frac{1}{2}w_o\left(\rho\vec{\nabla}\cdot\vec{J}+\rho_n\vec{\nabla}\cdot\vec{J}_n+\rho_p\vec{\nabla}\cdot\vec{J}_p\right), \quad (10)$$

where $\rho=\rho_n+\rho_p$, $\tau=\tau_n+\tau_p$, and $\vec{J}=\vec{J}_n+\vec{J}_p$. The direct part of the coulomb int-eraction in $H_C(\vec{r})$ is $\frac{1}{2}V_C(\vec{r})\rho_p(\vec{r})$, where

$$V_C(\vec{r})=\int\rho_p(\vec{r})\frac{e^2}{|\vec{r}-\vec{r}'|}d^3r'. \quad (11)$$

By comparing the terms proportional to t_o and t_3 in Eq. (10) one can see that the three-body contact interaction in second part of Eq. (1) is equivalent to the density-dependent two-body force. This equivalence, however, is valid only for the case we have investigated, namely that of an even-even nucleus.

The mean square radii for protons and neutrons are defined as (q=n or p) [9],

$$\langle r_q^2\rangle=\int_0^{R_{hw}}r^2\rho_q(\vec{r})d^3\vec{r}, \quad (12)$$

and the rms radii are simply given by

$$r_q=\langle r_q^2\rangle^{\frac{1}{2}}. \quad (13)$$

The mean square radius of the charge distribution in a nucleus can be expressed as:

$$\langle r_{ch}^2\rangle=\langle r_p^2\rangle+\langle r_{ch}^2\rangle_p+(N/Z)\langle r_{ch}^2\rangle_n+r_{cm}^2+r_{so}^2, \quad (14)$$

where $\langle r_p^2\rangle$ is the mean square radius of the point proton [Eq. (12)] and $\langle r_{ch}^2\rangle_p$ and $\langle r_{ch}^2\rangle_n$ arethe mean square charge radii of a proton and a neutron, respectively. The quantity r_{cm}^2 is a small correction due to the center-of-mass motion, which is evaluated assuming harmonic-oscillator wave functions. The last term r_{so}^2 is a tinyspin-orbit contribution to the charge density. Correspondingly, we define the charge rms radius as [9].

$$r_c=\langle r_{ch}^2\rangle^{1/2}, \quad (15)$$

An interesting phenomenon in nuclear structure is the formation of a skin of neutrons on the surface of a nucleus, and its evolution with mass number in an isotopic chain [10]. A precise measurement of the thickness of neutron skin is important not only because this quantity represents a basic nuclear property, but also because its value constrains the symmetry energy term of the nuclear equation of state [11]. A detailed knowledge of the symmetry energy is essential for describing the structure of neutron-rich nuclei, and for modeling properties of neutron-rich matter in applications relevant for nuclear astrophysics [12].

The thickness of a neutron skin in nuclei may be defined in different ways. One of these possibilities is to define it as the difference between the neutron and proton radii of the equivalent uniform spheres. Alternatively, it can be defined as the difference between the neutron and proton diffraction radii or Helm radii, in addition to that it's defined as the difference between the charge rms radius of neutrons and that of protons, as we have used in this work.

$$\Delta r_c=r_c(n)-r_c(p), \quad (16)$$

As we move away from closed shells, pairing correlations play an important role

and should be taken into account. Two different forms of pairing force, the volume type

$$V_{vol}^{\delta}(r,r') = V_o \delta(r - r') \quad (17)$$

or the surface type,

$$V_{surf}^{\delta}(r,r') = V_o \left[1 - \frac{\rho(r)}{\rho_o}\right] \delta(r - r'), \quad (18)$$

where $\rho_o = 0.16\ fm^{-3}$ is the saturation density, and V_o defines the strength of the interaction. The surface interaction gives the pairing gaps that increase very rapidly in light nuclei, while the volume force gives the values that are almost independent of A. The experimental data show the trend that is intermediate between surface and volume; hence, below we study the intermediate-character pairing force that is half way in between, i.e., it is defined as [13]:

$$V_{mix}^{\delta}(r,r') = \frac{1}{2}\left(V_{surf}^{\delta} + V_{vol}^{\delta}\right) = V_o \left[1 - \frac{\rho(r)}{2\rho_o}\right] \delta(r - r'). \quad (19)$$

Results and discussion

The ground-state proton and neutron densities are one of the most important properties of nuclei, due to the short-range nature of the strong interaction. The ground-state nuclear matter density of a nucleus serves as the MF in which the nucleons move. Therefore, many properties of a given nucleus are related to its ground-state proton and neutron densities. The density and the internal properties that discussed in this research was calculated by using the HFBRAD (v1.00) [14] program. (Which uses direct integration of the second-order HFB plus effective Skyrme interaction equations in a coordinate representation), where a standard iterative procedure is used to find self-consistent solutions for the nuclear wave functions and densities. Theoretically, the shape of the density distribution includes detailed information on the internal nuclear structure of the Sn isotopes is shown in Fig. 1. We show the proton and neutron density distributions $\rho_q(r)$ [Eq. (9)] of some selected isotopes in the Sn chain considered.

In the Fig.1, we have chosen two extreme neutron-deficient and neutron-rich isotopes and one stable isotope between them. We see the evolution of these densities as we increase the number of neutrons. For ^{100}Sn ($N = Z = 50$), we see that the two densities are practically the same except for Coulomb effects that make the protons to be more extended and, therefore, this has to be compensated with a small depression in the interior. The effect of adding more and more neutrons is to populate and extend the neutron densities. This also makes the proton distribution follow the neutron one, increasing its spatial extension. The cost of this radius enlargement in the case of protons is a depression in the nuclear interior to preserve the normalization to the constant number of protons $Z = 50$. Then, it can be seen graphically the emergence of a region at the surface where the protons have practically disappeared while the neutrons still survive.

On the theoretical side the difference between the neutrons and protons distribution Fig. 2 can be obtained in the framework of HF method (see for example [15]) or HFB method (see for example [16, 17]). As a rule of thumb, a theoretical calculation of the nuclear density is considered good when it reproduces the data on elastic electron scattering. But some details of the theoretical densities might not be accessible in the experiments, due to poor resolution or limited experimental reach of the momentum transfer q. We have seen that the density dependence of Skyrme's interaction allows a remarkable description of ground-state properties of doubly-closed shell nuclei.

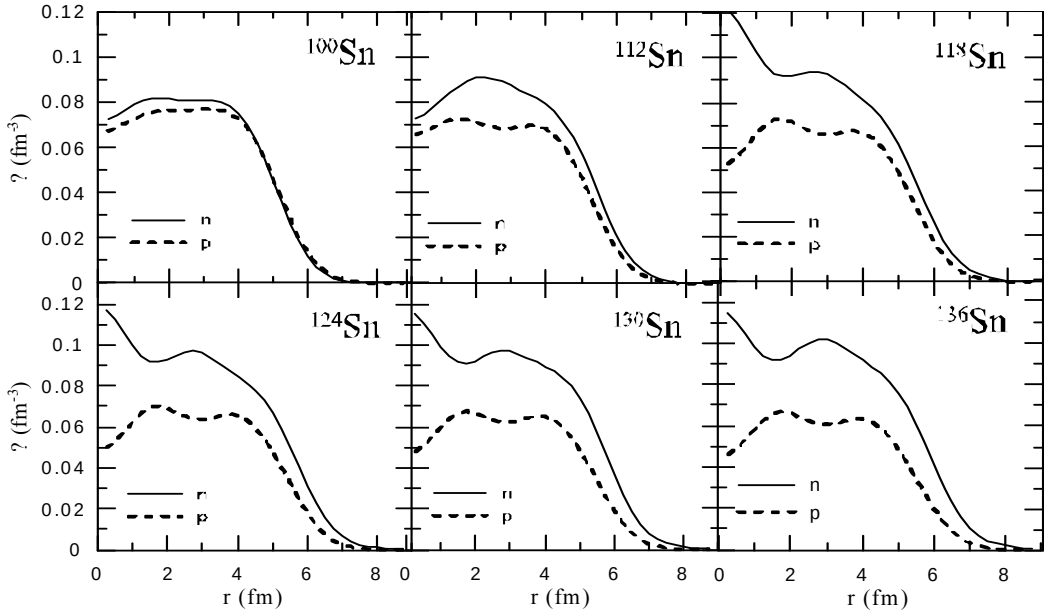

Fig. 1: Proton and neutron densities for some Tin isotopes calculated using SLy5 parameterization.

Over all, these results are even in better agreement with experiment than any HF calculations made with density dependent effective forces derived from Bruckner theory in the local-density approximation. They show that Skyrme's interaction provides, with only five parameters shown its values in Table 1, a very simple parameterization of the nuclear effective interaction, which already contains all the ingredients necessary to give a good description of the average nuclear field.

We show our results for the rms radii of the charge distributions [Eq. (15)].We compare them to the available experimental information obtained from various methods including laser and muonic atoms spectroscopy [18-22].We also compare between results with different theoretical force of Skyrme calculations. The SkM* is the closer force to the experimental data. The general purpose of Fig. 3 is to show that different Skyrme forces do not differ much in their predictions of charge rms radii then, by comparing our results with experiment and with other theoretical results, we have evaluated the quality of our calculations.

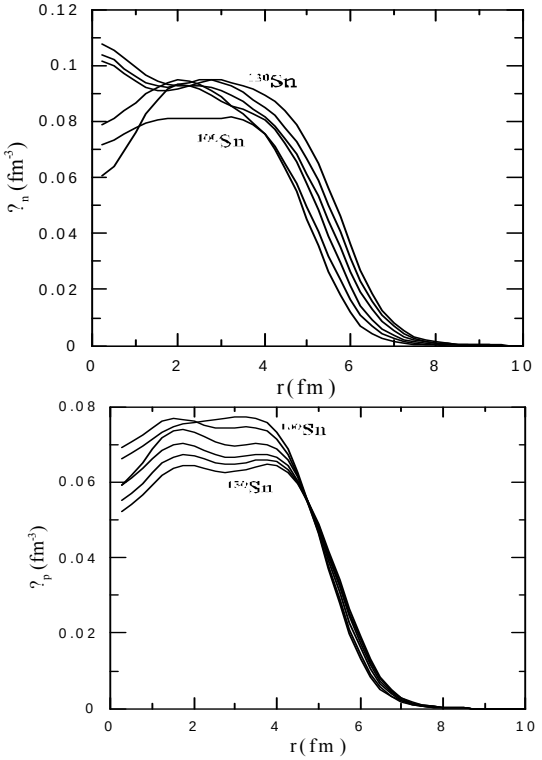

Fig. 2: Density of even-even Sn Isotopes using SkM* parameterization by increasing six steps. Left hand side: neutron density. Right hand side: proton density.

Table 1: Parameters in the particle–hole channel for the different versions of the Skyrme forces implemented in the program HFBRAD [14].

	SIII	SkM*	SLy4	SLy5
t_o	-1128.75	-2645.0	-2488.913	-2488.345
t_1	395.0	410.0	486.818	484.230
t_2	-95.0	-135.0	-546.395	-556.690
t_3	14000.0	15595.0	13777.0	13757.0
x_o	0.45	0.09	0.834	0.776
x_1	0.0	0.0	-0.344	-0.317
x_2	0.0	0.0	-1.000	-1.000
x_3	1.0	0.0	1.354	1.263
α	1.0	1/6	1/6	1/6
w_o	130.0	120.0	123.0	125.0

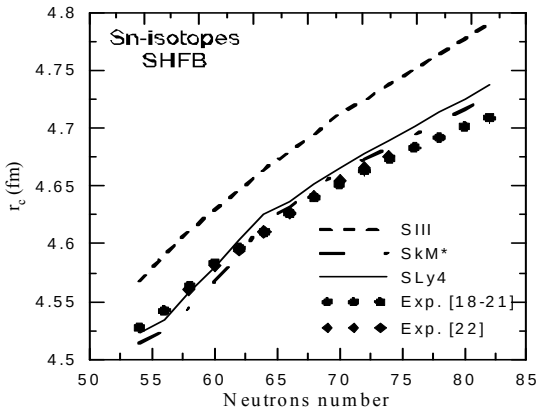

Fig. 3: Charge rms radii of Sn isotopes. The SLy4, SIII, and SkM* results are compared with Experimental data [18-22].

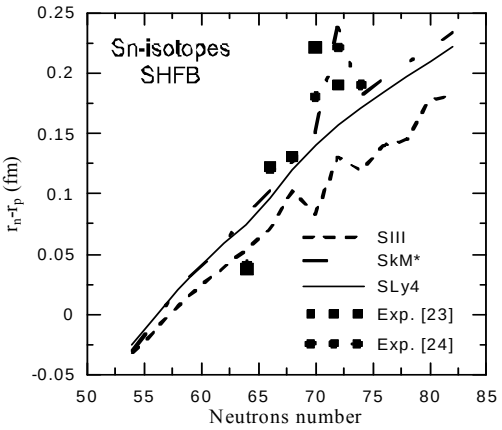

Fig. 4: Difference between neutron and proton charge rms radii of Sn isotopes. The SLy4, SIII, and SkM* results are compared with Experimental data [23, 24].

As mentioned previously, the thickness of a neutron skin in nuclei may be defined in different ways. One of these ways is to define it as the difference between the charge rms radius of neutrons and that of protons, as we have plotted in Fig. 4. The comparison between the calculated results (obtained by SkM*, SLy4 and SIII) and these of experimental data [23, 24] are demonstrated in Fig. 4. When the nucleus is deformed, the thickness of the neutron skin might depend on the direction. It is an interesting and natural question to ask whether the deformed densities give rise to a different skin size in the different directions. It is also interesting to know whether the emergence of the skin may be influenced by the nuclear shape. We study in this work such dependence in the case of Sn isotopes, which are examples of well-deformed nuclei characterized by a large variety of competing nuclear shapes [25]. In the present implementation, this is achieved by using the single-particle wave functions of the Transformed Harmonic Oscillator (THO), which allows for an accurate description of deformation effects and pairing correlations in nuclei arbitrarily close to the particle drip lines. The program HFBTHO [26], uses the axially THO single-particle basis to expand quasiparticle wave

functions. It iteratively diagonalizes the HFB Hamiltonian based on the Skyrme-forces and zero-range pairing interaction until a self-consistent solution is found the program used the SLy4 Skyrme parameterizations and the mixed pairing force Eq. (19). The results which we obtain for the binding energy of the selected Sn isotopes as a function of the quadrupole parameter $\beta = \sqrt{\pi/5}\, Q_p/(z r_p^2)$ ($Q_p$being the proton quadrupole moment) are presented (which called the potential energy curves (PECs)). In Figs. (5-a) and (5-b), as seen that the prolate shape appears in the semi magic number of ^{106,118}Sn but in Fig (5-c) the symmetry shape in^{130}Sn is seen because the neutron number of this isotopes is nearly the magic number.

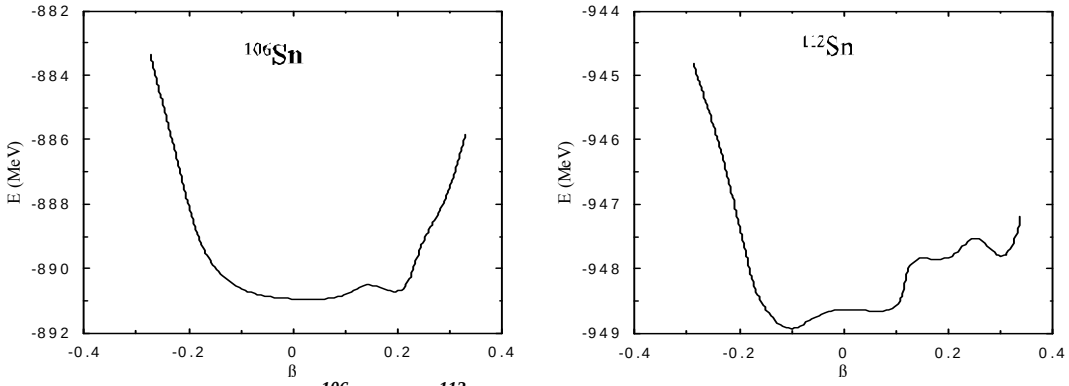

Fig.(5-a):PEC for ^{106}Sn and ^{112}Sn by HFB using SLy4 and mixed pairing force.

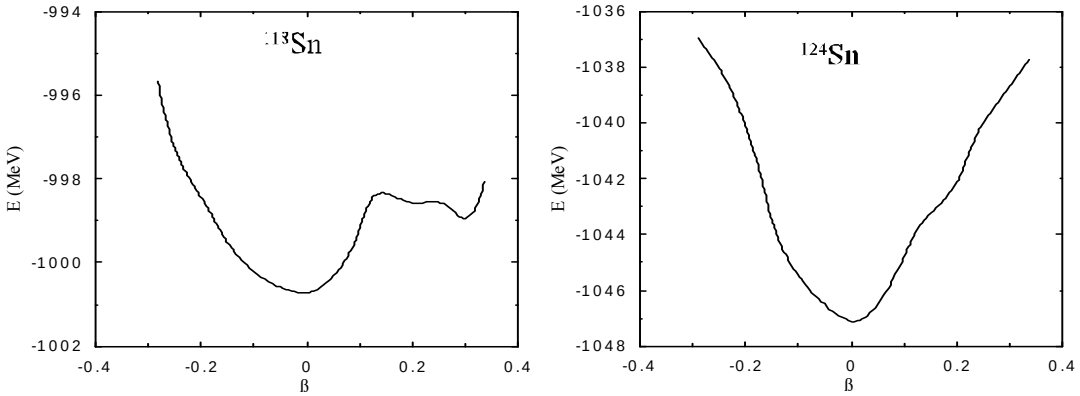

Fig. (5-b): PEC for ^{118}Sn and ^{124}Sn by HFB using SLy4 and mixed pairing force.

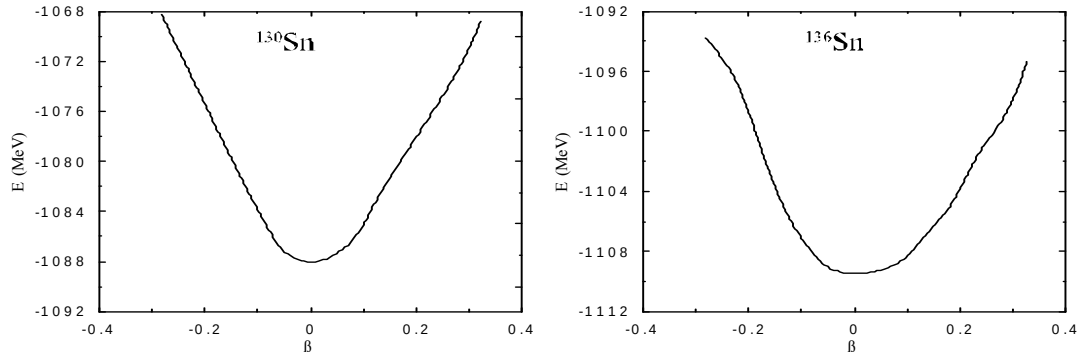

Fig. (5-c): PEC for ^{130}Sn and ^{136}Sn by HFB using SLy4 and mixed pairing force.

Conclusions

1- We conclude that our method reproduces the experimental data with accuracy similar to that of other microscopic calculations which may be more sophisticated but may also be more time consuming. This agreement provides a good starting point for making predictions of other quantities such as neutron-proton radii differences, where the experimental information is scarce and not as accurate as in the case of charge radii.
2- We conclude that the energy barriers in the PECs depend strongly on the details of calculations, especially on the pairing force.

References

[1] K. Bennaceur, P. Bonche, J. Meyer, C. R. Physique, 4 (2003) 555.
[2] J. dobaczewski, W. Nazarewicz, M. V. Stoitsov, Phys. Rev. C63 (2001) 024308.
[3] P. Ring, P. Schuck "The Nuclear Many-Body Problem" Spinger-Verlag, Berlin (1980).
[4] G. Bertsch, Z. Phys. A289 (1978) 103.
[5] D. Vautherin, Phys. Rev. C7 (1973) 296.
[6] D. Vautherin, D. M. Brink, Phy. Rev. C5, 3 (1972) 626.
[7] J. S. Bell, T. H. R. Skyrme, Phil. Mag. 1 (1956) 1055.
[8] E. B. Suckling "Nuclear Structure and Dynamics from the Fully Unrestricted Skyrme-Hartree-Fock Model" Ph.D. thesis, University of Surrey (2011).
[9] P. Sarriguren, M. K. Gaidarov, E. Moya de Guerra and A. N. Antonov Phy. Rev. C76 (2007) 044322.
[10] T. Suzuki, H. Geissel, O. Bochkarev, L. Chulkov, Phys. Rev. Lett. 75 (1995) 3241.
[11] S. Terashima, H. Sakaguchi, H. Takeda, T. Ishikawa, Phys. Rev. C77 (2008) 024317.
[12] J. Piekarewicz, B. K. Agrawal, W. Nazarewicz, P.-G. Reinhard, Phys. Rev. C85 (2012) 041302.
[13] A.V. Avdeenkov, S.P. Kamerdzhiev, JETP Letters 69 (1999) 715.
[14] K. Bennaceur, J. Dobaczewski, Comp. Phys. Comm. 168 (2005) 96.
[15] F. Hofmann, H. Lenske, Phys. Rev. C57 (1998) 2281.
[16] S. Mizutori, J. Dobaczewski, W. Nazarewicz, P.-G. Reinhard, Phys. Rev. C61 (2000) 044326.
[17] A. N. Antonov, D. N. Kadrev, M. K. Gaidarov, E. M. Guerra, Phys. Rev. C72 (2005) 044307.
[18] F. Le Blanc, L. Cabaret, J.E. Crawford, Eur. Phys. J. A15 (2002) 49.
[19] F. Le Blanc, L. Cabaret, E. Cottereau, Phys. Rev. C72 (2005) 034305.
[20] M. Anselment, K. Bekkand G. Schatz, Phys. Rev. C34 (1986) 1052.
[21] C. Piller, C. Gugler, J. Herberz, Phys. Rev. C42 (1990) 182.
[22] I. Angeli, At. Data Nucl. Data Tables 87 (2004) 185.
[23] L. Ray, Phys. Rev. C19 (1979) 1855.
[24] A. Trzcinska, J. Jastrzebski, B. Klos, Phys. Rev. Lett. 87 (2001) 082501.
[25] P. Sarriguren, E. Moya de Guerra, A. Escuderos, Phys. Rev. C64 (2001) 064306.
[26] M.V. Stoitsov, J. Dobaczewski, W. Nazarewicz, P. Ring, Comp. Phys. Comm.167 (2005) 43.